

Selective Chemical Modulation of Gene Transcription Favors Oligodendrocyte Lineage Progression

Mar Gacias,^{1,5} Guillermo Gerona-Navarro,^{2,3,5} Alexander N. Plotnikov,² Guangtao Zhang,² Lei Zeng,² Jasbir Kaur,¹ Gregory Moy,¹ Elena Rusinova,² Yoel Rodriguez,^{2,4} Bridget Matikainen,¹ Adam Vincek,² Jennifer Joshua,² Patrizia Casaccia,^{1,*} and Ming-Ming Zhou^{2,*}

¹Departments of Neuroscience and Genetics and Genomic Sciences

²Department of Structural and Chemical Biology

Icahn School of Medicine at Mount Sinai, 1425 Madison Avenue, New York, NY 10029, USA

³Department of Chemistry, Brooklyn College, 2900 Bedford Avenue, Room 351 NE, Brooklyn, NY 11210, USA

⁴Department of Natural Sciences, Hostos Community College of CUNY, Bronx, NY 10451, USA

⁵Co-first author

*Correspondence: patrizia.casaccia@mssm.edu (P.C.), ming-ming.zhou@mssm.edu (M.-M.Z.)

<http://dx.doi.org/10.1016/j.chembiol.2014.05.009>

SUMMARY

Lysine acetylation regulates gene expression through modulating protein-protein interactions in chromatin. Chemical inhibition of acetyl-lysine binding bromodomains of the major chromatin regulators BET (bromodomain and extraterminal domain) proteins has been shown to effectively block cell proliferation in cancer and inflammation. However, whether selective inhibition of individual BET bromodomains has distinctive functional consequences remains only partially understood. In this study, we show that selective chemical inhibition of the first bromodomain of BET proteins using our small-molecule inhibitor, Olinone, accelerated the progression of mouse primary oligodendrocyte progenitors toward differentiation, whereas inhibition of both bromodomains of BET proteins hindered differentiation. This effect was target specific, as it was not detected in cells treated with inactive analogs and independent of any effect on proliferation. Therefore, selective chemical modulation of individual bromodomains, rather than use of broad-based inhibitors, may enhance regenerative strategies in disorders characterized by myelin loss such as aging and neurodegeneration.

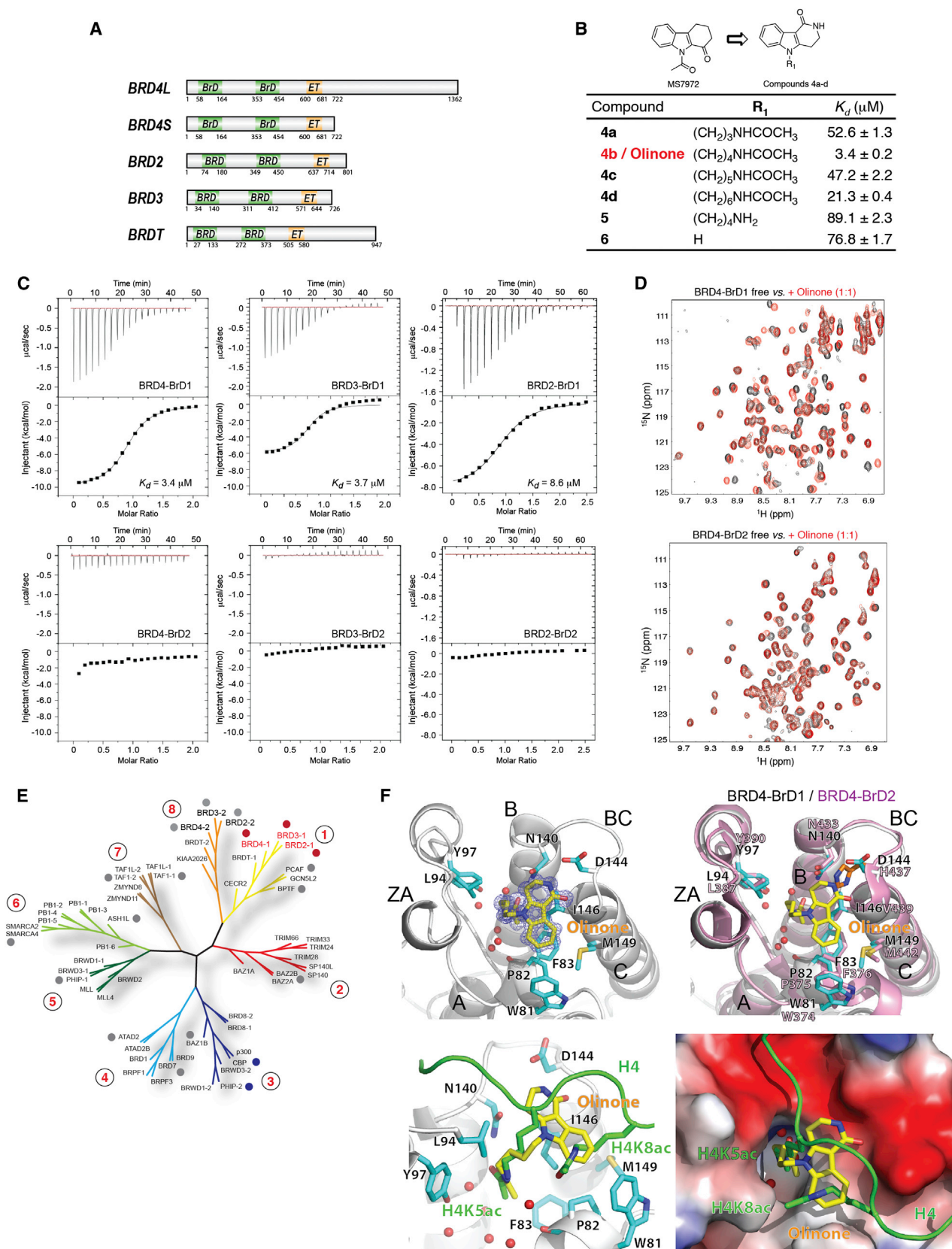
INTRODUCTION

Lysine acetylation plays an essential role in gene transcriptional regulation. The evolutionarily conserved bromodomain (BrD) functions as the acetyl-lysine binding domain (Dhalluin et al., 1999) for acetylated histones and transcription factors, which is required for ordered gene transcription in chromatin (Sanchez and Zhou, 2009). BRD4 is a representative member of the BET (bromodomain and extraterminal domain) family of proteins, characterized by two tandem BrDs (BrD1 and BrD2) followed by an extraterminal domain. Through its BrD/acetyl-lysine binding, BRD4 functions to facilitate recruitment of transcription fac-

tors to target genes, assembly of the mediator complex at enhancer sites, and activation of paused RNA polymerase II complexes for productive transcriptional elongation (Chiang, 2009). Numerous studies have reported that broad chemical inhibition of both BET BrDs effectively blocked genome-wide transcription. This was particularly true for genes regulating proliferation of cancer cells, including NUT midline carcinoma (Filippakopoulos et al., 2010), acute myeloid leukemia (Zuber et al., 2011), MLL-fusion leukemia (Dawson et al., 2011), and neuroblastoma (Puissant et al., 2013). It was also suggested that by modulating gene transcription in immune cells, BrD inhibition has a therapeutic role in inflammatory diseases (Nico-deme et al., 2010; Zhang et al., 2012a). However, the use of selective inhibitors of single BrDs could have distinctive functional features.

We addressed this question in oligodendrocyte lineage cells, the myelin-forming cells of the central nervous system whose differentiation has been previously shown to require cell-cycle exit (Casaccia-Bonnel and Liu, 2003; He et al., 2007; Magri et al., 2014a, 2014b) and histone deacetylase activity (Marin-Husstege et al., 2002; He et al., 2007; Shen et al., 2008). In this lineage, the early progenitor stage is characterized by global protein lysine acetylation and decreased global histone acetylation, previously identified as critical for the proper onset of oligodendrocyte differentiation (Shen et al., 2008; Wu et al., 2012; Ye et al., 2009). Therefore, we reasoned that oligodendrocyte lineage cells would be a suitable biological system to test the functional consequences of BET protein BrD inhibition using chemical inhibitors selective for only one or both BrDs of BET proteins.

Notably, previous studies have reported distinctive functions of the two BrDs of BET proteins, possibly consequent to the interaction with lysine-acetylated histones or with transcriptional proteins (Gamsjaeger et al., 2011; Huang et al., 2009; Jang et al., 2005; Lamonica et al., 2011; Schröder et al., 2012; Shi et al., 2014; Yang et al., 2005; Zhang et al., 2012a). In the case of human BRD4, the first BrD appears dedicated to anchoring this molecule and its associated proteins to target gene promoter and enhancer sites in chromatin, through binding to diacetylated H4K5ac/K8ac (a mark for gene transcriptional activation), while the second BrD was associated with the recruitment of nonhistone proteins (i.e., transcription factors and the pTEFb complex) to target genes. In the case of BRD3, however, it is the first BrD



(legend on next page)

that binds to the hematopoietic transcription factor GATA1 (Gamsjaeger et al., 2011; Lamonica et al., 2011), thereby suggesting context-dependent different functions of the two BrDs of the BET proteins in the regulation of ordered gene transcription in chromatin.

This distinctive and unique ligand-binding selectivity of the two BrDs has been attributed to a few amino acid residues that distinguish the first and second BrDs within each BET protein, while they all share nearly identical residues at the corresponding acetyl-lysine binding pocket. In an effort to understand specific molecular functions of the individual BrDs of BET proteins, we developed small-molecule chemical inhibitors that are capable of selectively modulating acetyl-lysine binding activity of the first and/or second BrDs of BET proteins and evaluated their effects on the progression of oligodendrocyte progenitor cells (OPCs) toward differentiation.

RESULTS AND DISCUSSION

Structure-Guided Development of the Selective BET BrD Inhibitor Olinone

We used a structure-guided design strategy to develop selective small-molecule inhibitors for the BET BrDs (Figure 1A). Our rational design of BET-specific BrD inhibitors (BrDis) started with a chemical scaffold of tetrahydro-pyrido indole that was present in a nuclear magnetic resonance (NMR)-based screen hit (MS7972) and showed modest activity as an inhibitor of the CBP BrD (Figure 1B) (Sachchidanand et al., 2006). This chemical scaffold is amenable to varying chemical modifications that can be synthetically added on to optimize its interactions with a target protein. Guided by the structural insights of MS7972 bound to the CBP BrD, we designed a series of 1-substituted-2,3,4,5-tetrahydro-pyrido-[4,3-b]indol-1-ones as inhibitors for the BET BrDs. These molecules extend from the key features present on MS7972 for the binding to the BET BrDs to contain a longer acetamidoalkyl substituent at the *N*-indole as well as an endocyclic peptide bond to enhance interactions with the BrDs (Figure 1B).

The synthesis of these compounds was achieved in four steps (see Figure S1 available online). Phenylhydrazone 1 was prepared by reaction of phenylhydrazine with 2,4-piperidinedione in water (with 10% acetic acid) under nitrogen atmosphere. Next, the pyrido-indole scaffold was constructed by Fisher

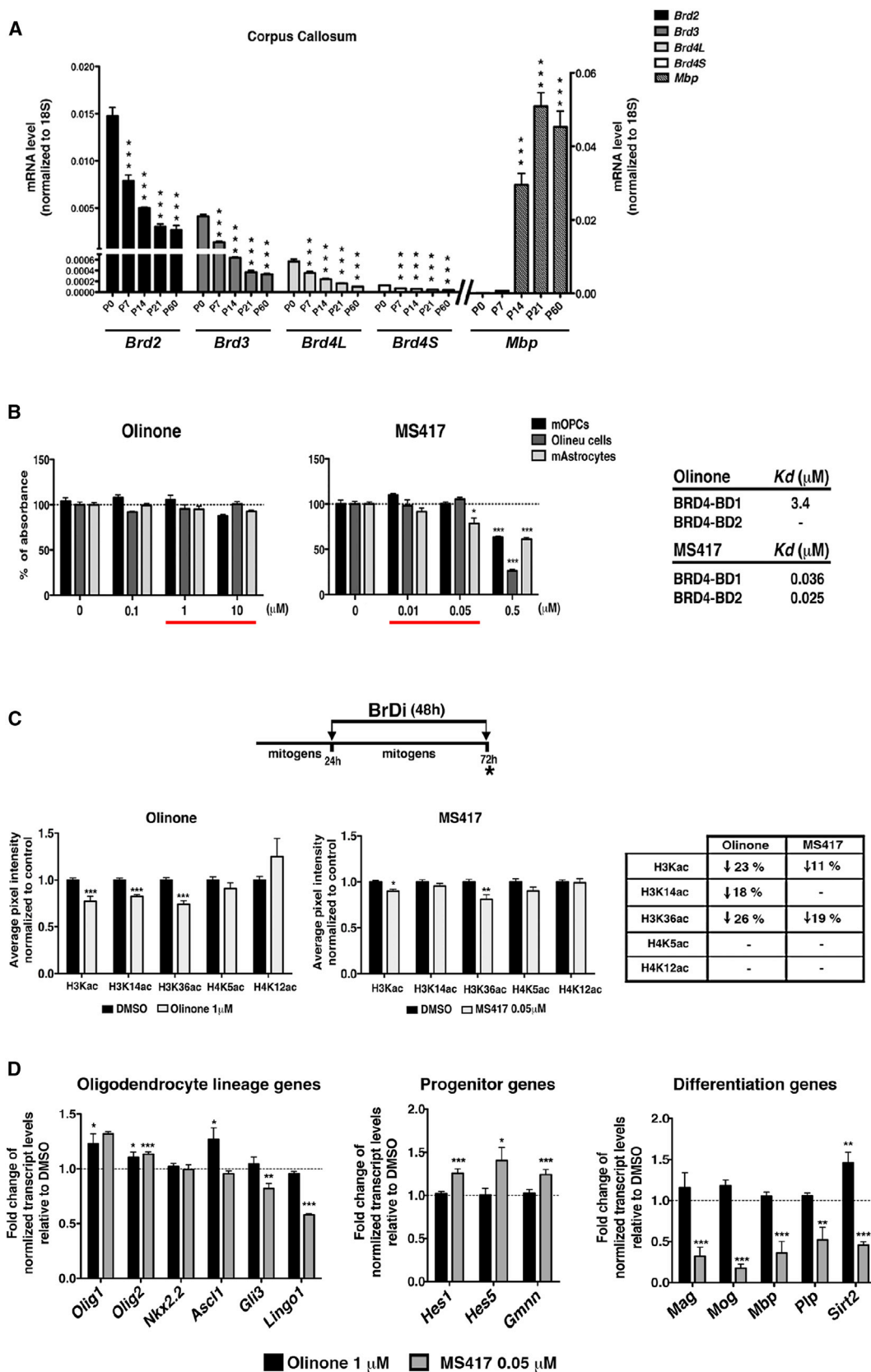
indole synthesis from treatment of phenylhydrazone 1 with sulfuric acid (70%) at 0°C (Rodriguez and Temprano, 1989). The resultant 2,3,4,5-tetrahydro-1H-pyrido-[4,3-b]indol-1-one 2 was *N*-alkylated with a corresponding phthalimido protected alkyl bromide in the presence of lithium bis(trimethylsilyl) amide as a base (Coldham et al., 2007). Finally, treatment of *N*-phthalimido protected substituted pyrido-indoles with hydrazine hydrate and subsequent acetylation afforded the final compounds 4a to 4d with good yields. Similar procedures were used to generate compounds 5 and 6 (Figure 1B).

We assessed binding affinity of 4a to 4d, 5, and 6 to BrDs of BET proteins by using isothermal titration calorimetry (ITC) (Figure 1C; Figure S2A). The structure-activity relationship data revealed that the length of the *N*-alkylated chain plays an important role in binding to BRD4-BrD1. An *N*-alkylated chain of four methylene units as in 4b seems to be optimal in binding to BRD4-BrD1, with a binding dissociation constant K_d of 3.4 μ M. This represents a greater than 15-fold improvement in binding affinity compared with those analogs that comprise three, five, or six methylene groups (i.e., 4a, 4c, and 4d, respectively) (Figure 1B). Furthermore, elimination of the acetyl group (5) or the entire *N*-acetylated group (6) resulted in a dramatic loss in binding affinity. We named the best compound of the series 4b Olinone for its cellular activity as described below. Consistently, we observed that Olinone exhibits preferred binding for the BrD1 over the BrD2 from all three BET proteins BRD4, BRD3, and BRD2, as assessed by ITC measurements (Figure 1C).

We next profiled Olinone binding selectivity to different BrDs using 2D ^1H - ^{15}N heteronuclear single-quantum coherence (HSQC) NMR spectroscopy (Figure 1D; Figure S2B). The NMR method offers a reliable assessment for ligands that bind to target proteins with tens to hundreds micromolar affinity, which is complementary to ITC, which allows quantitative measurements of ligand binding in low-micromolar affinity. Notably, Olinone showed modest binding to the BrDs from CBP and PHIP, with K_d values of 33 and 103.4 μ M, respectively; very weak binding to BRD4-BrD2, with $K_d > 300 \mu$ M; and almost no detectable binding to the BrDs from many other proteins, including BRD7, PCAF, ASH1L, TAF1L, SMARCA4, BAZ1B, BAZ2B, ATAD2, BPTF, and TRIM24, which represent different subgroups of the human BrD family (Figure 1E; Figure S2C). The selectivity for the BrD1 over the BrD2 of the BET proteins was further confirmed using a fluorescence anisotropy competition binding assay (Figure S2D).

Figure 1. Structure-Guided Design of Olinone, a Selective Inhibitor for the BET BrD1

- (A) Schematic illustration of domain organization of the members of the BET protein family. ET, extraterminal domain.
 (B) Structure and binding affinity of Olinone and its analogs for the BRD4-BrD1, determined by using ITC. Results are representative of three independent experiments, and the error is the SD.
 (C) ITC determination of binding affinity of Olinone to the two individual BrDs of BRD4, BRD3, and BRD2.
 (D) Selectivity binding of Olinone to BRD4-BrD1 versus BRD4-BrD2, as illustrated by 2D ^1H - ^{15}N HSQC spectra of a given BrD in the free form (black) and in the presence of Olinone (red), as well as by ITC.
 (E) Phylogenetic tree of the human BrD family. Dots indicate the BrDs for which Olinone binding affinity was evaluated in the assay described in (B) and (C). Dots are color coded for high affinity (red), modest affinity (blue), or no binding (gray).
 (F) Structural basis of selective binding of Olinone to BRD4-BrD1. Upper left: Crystal structure of Olinone (yellow) bound to BRD4-BrD1, depicted in a ribbon diagram. The Fo-Fc electron density map was computed after simulated annealing with the compound omitted from the atomic model and shown in blue mesh (contoured to 1.0 σ). Upper right: Structural comparison of BRD4-BrD1 and BRD4-BrD2 (PDB accession number 2YEM), showing steric clash between Olinone with His437 in BRD4-BrD2. Lower left and right: Superimposition of crystal structures revealing how Olinone (yellow) and an H4K5ac/K8ac peptide (green) are bound to the BRD4-BrD1 in the protein/ligand complex, depicted in ribbon diagram or electrostatic surface representation (right). Side chains of key amino acid residues at the ligand-binding site in the protein are color coded by atom type, and bound water molecules are shown as red spheres.
 See also Figures S1 and S2 and Table S1.



(legend on next page)

Moreover, through characterization of Olinone binding to a set of wild-type or acetyl-lysine binding-deficient mutants of the tandem BrDs of BRD4 proteins, we observed that the two BET BrDs function almost independently of each other, consistent with a long linker sequence that connects them (Figure S2D). Collectively, these results demonstrate that Olinone is a highly selective inhibitor against the first BrD of the BET proteins.

Molecular Basis of Selective Recognition of BRD4 BrD1 by Olinone

The molecular basis of Olinone recognition of the BrD1 of BET proteins was revealed by our X-ray crystal structure of the BRD4 BrD1/Olinone complex, determined at 0.94 Å resolution (Table S1). Olinone forms a chairlike conformation in the bound state (Figure 1F, upper left), its triheterocyclic moiety as the seat packs against the side chains of Trp81 and Pro82 in the one-turn helix Z', and Ile146 in helix C, and interacts with Asp144 at the opening of the acetyl-lysine binding pocket formed between the ZA and BC loops. Asp144 is one of a few residues that are different between BRD4-BrD1 and BrD2 in the acetyl-lysine binding site; its corresponding residue in BrD2 is His437, which would clash with the indole moiety of Olinone (Figure 1F, upper right).

This major contribution to the overall ligand binding by Asp144 was confirmed in our detailed structural analysis of the BRD4-BrD1/Olinone complex. The acetyl chain of Olinone, as its back, intercalates into a hydrophobic pocket lined with Val87, Leu92, Leu94, and Tyr139 of the ZA loop. The carbonyl oxygen of the acetyl group of Olinone forms a hydrogen bond (2.9 Å) to the amide nitrogen of the highly conserved Asn140 in BRD4-BrD1. Notably, the acetyl chain of Olinone adopted an almost identical conformation and position as that of the acetylated-K5 side chain of histone H4K5ac/K8ac peptide when bound in BRD4-BrD1, whereas the piperidone ring of Olinone filled the site for K8ac binding in the H4 peptide (Figure 1F, lower left and right). This explains the optimal length of the acetyl side chain of Olinone in its chemical series and Olinone's effective inhibition of BRD4-BrD1 binding to the diacetylated H4K5ac/K8ac peptide. The binding affinity of the latter interaction, which is important for BRD4 functions in gene transcriptional regulation (Chiang, 2009; Filippakopoulos et al., 2012), is estimated to be a K_i of 26 μ M. Given that a few ligand-binding residues in BRD4-BrD1, such as Ile146 and Asp144, are not conserved outside the BET proteins in the human BrD family proteins (Sanchez and Zhou, 2009), this structure explains how Olinone is

selective for the first BrD of the BET proteins over other BrDs from different transcriptional proteins.

It is important to note that Olinone has superior selectivity between the two BrDs of BET proteins, even as compared with the recently developed MS436, a diazobenzene compound (Zhang et al., 2013), or the BET-specific BrDi MS417, which is a thienotriazolo-diazepine compound (Zhang et al., 2012b) and structurally related to (+)-JQ1 (Filippakopoulos et al., 2010) and I-BET (Nicodeme et al., 2010). These BET-specific BrDis, particularly MS417 and (+)-JQ1, have high affinity for BrD ($K_d = 20\text{--}100$ nM) but do not discriminate between the first and second BrDis of the BET proteins, because of greater than 95% sequence identity at the acetyl-lysine binding pocket.

Selective BET-BrD1 Inhibition Favors, whereas Broad BET BrD Inhibition Prevents the Differentiation of Oligodendrocyte Progenitors

To begin evaluating the differential effects of selective inhibitors of the first BrD (such as Olinone) and compare them with those of broad BET inhibitors (i.e., MS417 and JQ1), we measured the levels of expression of the BET protein-encoding genes in the developing white matter tracts of the mouse brain. Of the analyzed molecules, *Brd2* was the most abundant BET transcript in the neonatal brain (Figure 2A). However, it is worth noting that the levels of all the BETs (i.e., *Brd3*, *Brd4* long isoform, and *Brd4* short isoform) progressively declined in developing white matter tracts during a temporal window that was coincident with the differentiation of progenitors into myelin-forming oligodendrocytes, as detected by the expression of the myelin gene *Mbp* (Figure 2A).

To assess the ability of Olinone to modulate oligodendrocyte progenitor differentiation in mouse cultures, we first determined the effect of Olinone and MS417 on cell viability after 72 hr of treatment with increasing concentrations of BrDi, using a 1-methyl-1 H-tetrazole-5-thiol (MTT) assay (Figure 2B). No significant cytotoxicity was observed for Olinone or its inactive analog compound 5, up to a concentration of 10 μ M. In contrast, treatment with MS417 was toxic at doses of 500 nM and above (Figure 2B). Therefore, we opted to use Olinone at 1 μ M and MS417 at 0.05 μ M for most of the cellular studies.

We had previously reported that global histone acetylation characterizes proliferating progenitors and that deacetylation is necessary to initiate a differentiation program (Marin-Husstege et al., 2002; Shen et al., 2005). We therefore asked whether treatment with the BrD1 specific inhibitor Olinone or with the

Figure 2. Developmental Expression of BET Family Members in Corpus Callosum and Characterization of BrD Inhibition Effect in Oligodendroglial Cells

(A) Quantitative RT-PCR showing the transcript levels of *Brd2*, *Brd3*, and *Brd4-long* and *Brd4-short* isoforms in developing corpus callosum relative to 18S expression ($n = 3$ animals per age group; one-way ANOVA with Bonferroni posttest, *** $p < 0.01$ versus P0).

(B) MTT assay to measure cell viability in primary cultured mOPCs, primary cultured mouse astrocytes, and Olineu cells after 72 hr of treatment with BrDi at indicated doses (μ M). Red lines indicate the dose range matching with the K_d values of the inhibitors, showing no toxicity at the indicated concentrations. Right: Olinone and MS417 K_d values for the first and second BrDs of BRD4 ($n = 3$; one-way ANOVA with Dunnett's posttest, * $p < 0.05$, *** $p < 0.001$).

(C) Selective BET-BrD inhibition decreases histone acetylation. Top: experimental timeline. Bottom: automated high-throughput confocal screening for histone acetylation. The graph shows the quantification of the average nuclear residue-specific histone acetylation staining intensity in reference to DMSO ($n = 20$ sections; $n = 3$) (two-tailed t test, ** $p < 0.01$, *** $p < 0.001$). Error bars show \pm SEM.

(D) Effect of selective BET-BrD inhibition during the early differentiation phase of mOPCs. qRT-PCR showing the expression levels of differentiation markers after 24 hr of BrDi treatment (Olinone at 1 μ M and MS417 at 0.05 μ M). Results were normalized to Gapdh with relative mRNA levels in DMSO-treated control cells set to 1 ($n = 4$; one-way ANOVA with Dunnett's posttest, *** $p < 0.001$).

See also Figure S3, and Table S2.

BrD1/BrD2 inhibitor MS417 would similarly affect histone acetylation and gene transcription in immortalized oligodendrocyte progenitors (*Olineu*). The first experiment was conducted in the presence of mitogens, which represent a strong stimulus toward the persistence of global acetylation in these cells (Wu et al., 2012). Interestingly, in these cells, Olinone treatment resulted in an average reduction of histone H3 global acetylation, detected primarily at residues H3K14ac and H3K36ac, with little changes at H4K5ac and H4K12ac (Figure 2C). Treatment with MS417, in contrast, was less effective at reducing the histone acetylation levels at H3K14, although it decreased the levels of H3K36ac (Figure 2C). Despite the similar effect on histone deacetylation and on the expression of oligodendrocyte specific genes (Figure 2D), treatment of cells with Olinone consistently increased the transcript levels of myelin genes associated with the differentiated phenotype, whereas treatment with MS417 decreased the levels of these genes while increasing transcripts characteristic of the progenitor stage (Figure 2D). These results suggested that BrD1-specific inhibition promoted differentiation, whereas inhibition of both BrD1 and BrD2 prevented it and retained the cells at a progenitor stage.

Because an obligatory relationship exists between cell-cycle exit and differentiation in oligodendrocyte lineage cells (Swiss and Casaccia, 2010), and BrDis have been reported to inhibit proliferation of cancer cells, we asked whether the differential effect on differentiation observed after treatment with Olinone or MS417 could be due to a distinct modulation of the cell cycle. To address this question, we adopted three different approaches: immunohistochemistry with antibodies for the cell-cycle marker Ki67 (Figure 3A), expression levels of cell-cycle genes (Figure 3B), and fluorescence-activated cell sorting (FACS) analysis (Figure 3C). A detailed quantification of Olinone- or MS417-treated cells using immunoreactivity for Ki67 in order to identify proliferating cells did not reveal any difference among treatment groups (Figure 3A). Gene expression data analysis revealed an overall interesting effect of MS417, but not Olinone, on the transcript levels of cell-cycle genes (Figure 3B). Consistent with the inhibitory effect of MS 417, treatment with this broad BET inhibitor decreased the expression of the gene encoding for p21Waf1, which had been previously shown to positively affect oligodendrocyte differentiation (Zezula et al., 2001) while increasing the levels of cell-cycle genes preventing differentiation, such as E2F1 (Magri et al., 2014b) and c-Myc (Magri et al., 2014a). Finally, a measure of the DNA content by FACS analysis did not reveal significant differences in the relative proportion of cells in the different stages of the cell cycle (Figure 3C). Taken together, these data suggest that the prodifferentiation effect of the BrD1 inhibitor Olinone could not be interpreted as the consequence of precocious cell-cycle exit.

Temporal Control of BrDi Effectiveness on Oligodendrocyte Progenitor Differentiation

To gain a better understanding of the effect of the BrD1-specific or broad BET BrDis on differentiation, we conducted a dose-response experiment and measured the transcript levels of late differentiation genes. In both cases, we detected a dose-dependent response, corresponding to either MS417-mediated decrease or Olinone-induced increase of myelin gene transcripts at a dose comparable with the *in vitro* binding affinity to the

individual BrDs of BET proteins. This effect was clearly detectable as early as the first 24 hr of differentiation (Figure S3).

To further determine the window of effectiveness of BrDi treatment, we treated cells with either Olinone or MS417 for different amount of time in the presence of mitogens or in their absence. A 24 hr treatment in the presence of mitogens was not sufficient to detect the effects of MS417 or Olinone (Figure 4A). In contrast, treatment for 72 hr starting after the removal of mitogens was sufficient to alter the expression of the late differentiation genes (Figure 4B). Thus, inhibition of BrD binding was not sufficient to remove the inhibitory block of differentiation caused by mitogen stimulation and was detected only after the cells exited the cell cycle. The first 24 hr following cell-cycle exit represents an important critical window for the onset of a complex transcriptional program of differentiation. We therefore asked whether BrD inhibition during this critical period was sufficient to induce long-lasting changes. For this reason, after the first 24 hr of treatment, we washed out the drugs and allowed the cells to recover in differentiation medium (DM) prior to measuring the transcript levels of differentiation genes (Figure 4B). In these conditions, the levels of gene transcripts measured after washout did not reveal any change, which indicated that the effect of blocking BrDs was not stable but reversible over time.

The next question was to define whether inhibition of one or both BrDis would also be detected if cells were treated after the program of oligodendrocyte differentiation had started (i.e., after at least 48 hr in mitogen-free DM) (Figure 4C). In this case, the broad BET inhibition by MS417 still significantly decreased the expression of late differentiation genes, though to a lesser extent than continuous treatment, while the prodifferentiation effect of blocking only the first BrD1 by Olinone was dramatically reduced, with the exception of *Mog* levels (Figure 4C). Collectively, these data suggest that BET activity in oligodendrocyte lineage cells is differentially affected by inhibitors of the first BrD1 or of both BrDs of BET proteins.

Specificity and Off-Target Effects

We then examined the specificity of the effect of BrDi on oligodendrocyte differentiation by treating progenitors with structurally related but inactive compounds and conducted a detailed immunophenotypic (Figure 5A) and transcriptional (Figure 5B) characterization of mouse primary oligodendrocyte progenitor differentiation. Immunoreactivity for the proteoglycan NG2 was used to identify early progenitors, O4 to label cells expressing lipid sulfatides at an intermediate stage of maturation, and myelin basic protein (MBP) to identify differentiated oligodendrocytes. In untreated cultures, the progression of progenitors to mature oligodendrocytes was characterized by the progressive decrease of NG2 and the gradual acquisition of O4 immunoreactivity, followed by the acquisition of a myelinating phenotype, characterized by the extension of myelin membranes recognized by both O4 and MBP antibodies.

Treatment of primary oligodendrocyte progenitors with the BrD1-specific inhibitor Olinone promoted a shift toward the differentiated phenotype, as documented by the increased percentage of O4+ cells (Figure 5B), compared with DMSO-treated cells. This effect was not detected in cells that were treated with the inactive Olinone analog compound 5. Treatment of primary oligodendrocyte progenitors in the exact same conditions with

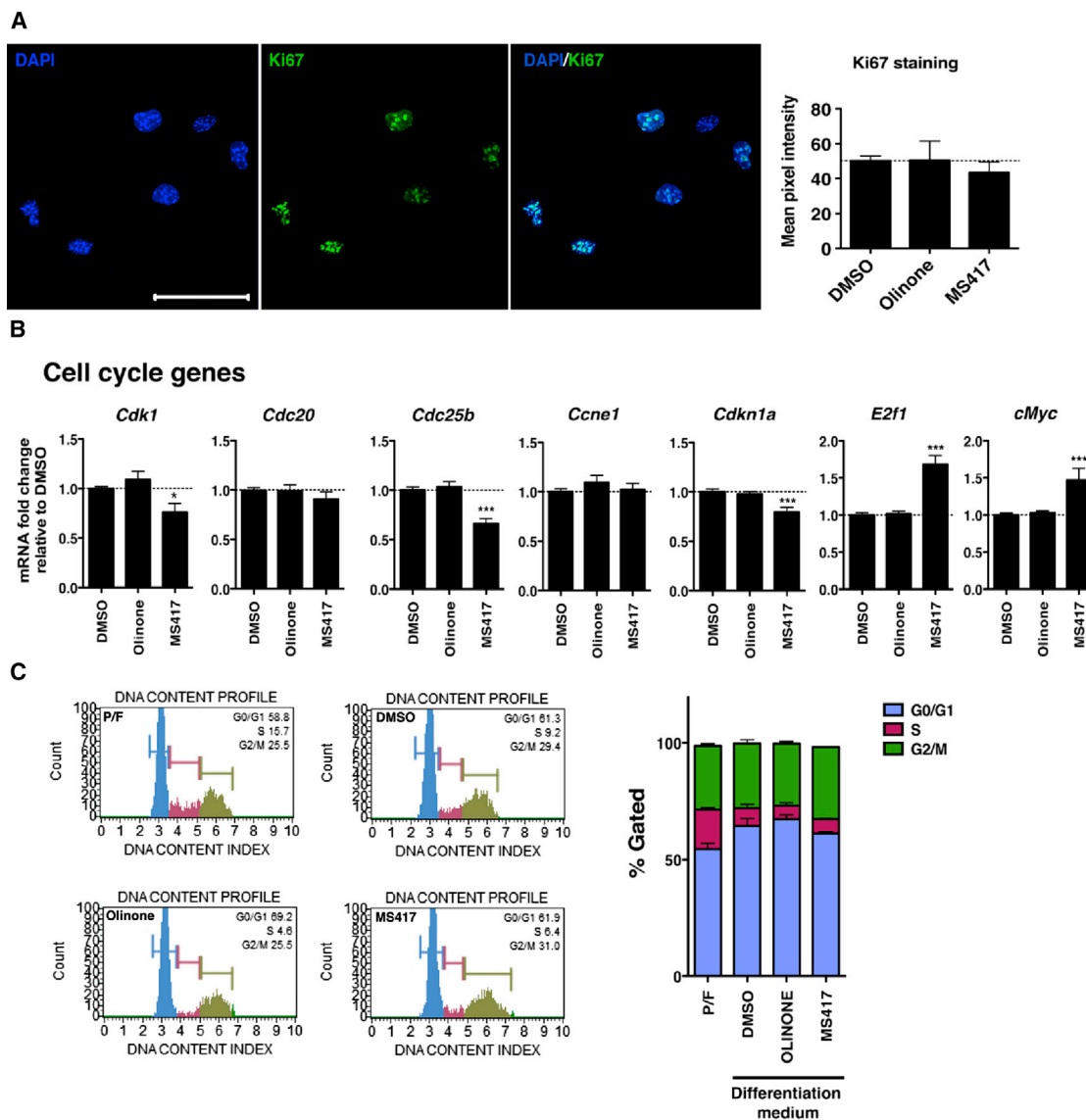


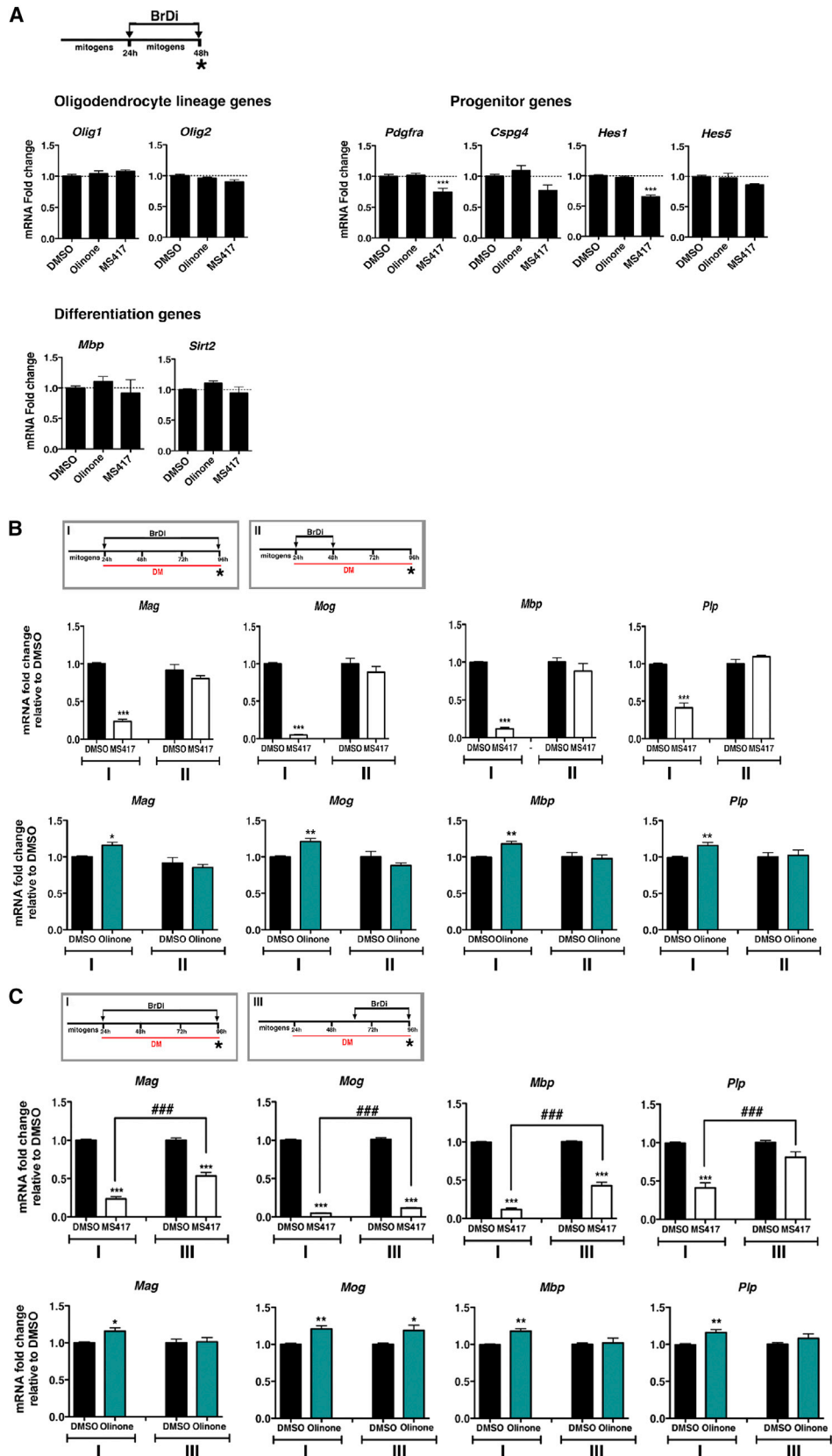
Figure 3. Treatment with BrDi Does Not Affect the Proliferation of Primary Cultured mOPCs and Cell-Cycle Exit upon Differentiation Stimuli
 (A) Representative confocal images of proliferating mOPCs stained with Ki67 antibody (green) and DAPI (blue). The scale bar represents 50 μ m. The graph represents the percentage of mean pixel intensity. Results shown are relative DMSO-treated control cells (set to 100%) ($n = 3$; one-way ANOVA with Dunnett's posttest).
 (B) qRT-PCR showing the expression levels of cell-cycle genes after 24 hr of BrDi (Olinone at 1μ M and MS417 at 0.05μ M). Results were normalized to *Gapdh*, with relative mRNA levels in DMSO-treated control cells set to 1 ($n = 3$; one-way ANOVA with Dunnett's posttest, $***p < 0.001$). Error bars show \pm SEM.
 (C) Cell-cycle analysis of BrDi-treated mOPCs for 24 hr as indicated. Color bars represent percentage of cells in each cell-cycle phase ($n = 2$; two-tailed t test). Error bars show \pm SEM.

the broader BET inhibitor MS417, in contrast, generated consistently opposite effects to those induced by Olinone. MS417 antagonized the progression toward a mature phenotype and reduced the number of NG2+/*O4*+ cells (Figure 5B). The effect was highly specific as the inactive enantiomer of MS417 (Zhang et al., 2012a), called MS566, was incapable of eliciting the same biological effect (Figure 5B). At a transcriptional level, the pro-differentiation effect of Olinone, but not compound 5, was also detected by the increased transcript levels for the late-differentiation markers *Mag*, *Mog*, *Plp*, and *Mbp* (Figure 5C), whereas MS417 treatment decreased the expression of these late-differ-

entiation markers in a dose-dependent fashion while increasing the expression of the transcriptional inhibitor of myelin genes, *Hes5* (Figure 5C).

Selective Inhibition of the BrD1 Enhances, whereas Inhibition of Both BET BrDs Prevents the Differentiation of Oligodendrocyte Progenitors

To begin to understand whether the inhibitory effect of MS 417 was consequent to the inhibition of both BrDs of BET proteins, we used two distinct approaches. First, we asked whether Brd2 in cultured progenitors was also the most prominent BET



(legend on next page)

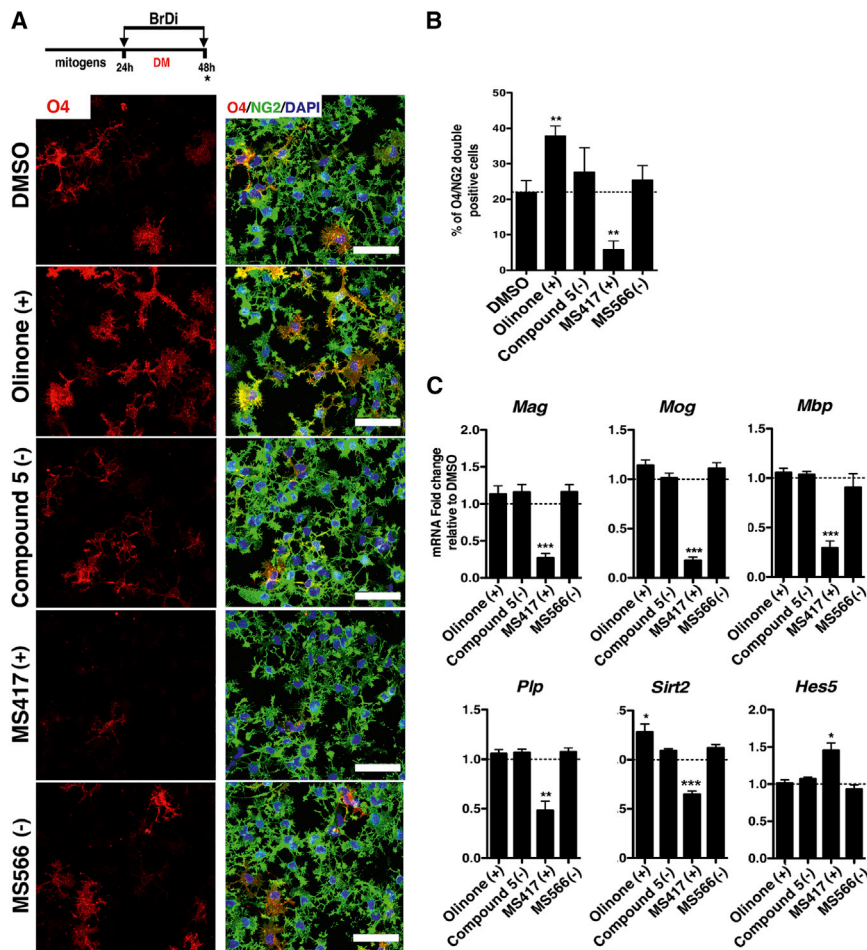


Figure 5. Olinone Specifically Promotes the Expression of the Oligodendrocyte Intermediate Differentiation Marker O4

(A) Top: experimental timeline. Bottom: confocal image of mOPCs treated for 24 hr with DMSO, Olinone (1 μ M), compound 5 (1 μ M), MS417 (0.05 μ M), and MS566 (0.05 μ M) in DM and stained with NG2 (green), O4 (red) antibodies, and DAPI (blue). The scale bar represents 50 μ m.

(B) Graph showing the quantification of the percentage of NG2+/O4+ staining in treated cells relative to DMSO ($n = 5-7$ sections per condition, $n = 3$ independent experiments; one-way ANOVA with Dunnett's post test, ** $p < 0.01$).

(C) qRT-PCR showing the expression levels of differentiation markers after 24 hr of BrDi (Olinone at 1 μ M, compound 5 at 1 μ M, MS417 at 0.05 μ M, MS566 at 0.05 μ M). Results were normalized to *Gapdh*, with relative mRNA levels in DMSO-treated control cells set to 1 ($n = 4$; one-way ANOVA with Dunnett's posttest, *** $p < 0.001$).

protein to be detected in the oligodendrocyte lineage cells (Figure 6A), which was consistent with our *in vivo* studies in developing myelinating tracts (Figure 2A). We then expressed either a wild-type EGFP-tagged Brd2 (EGFP-Brd2wt) molecule or a mutant form of Brd2 (EGFP-Brd2mut) lacking the acetyl-lysine binding domains in the first and second BrD of the protein molecule (Hnilicová et al., 2013) in *Olineu* cells and asked whether the two molecules were differentially distributed within the nuclei of transfected cells. Although the EGFP-Brd2wt transfected cells were characterized by a nuclear diffuse distribution, those transfected with the mutant eGFP-Brd2mut, lacking the ability to bind acetyl-lysine, showed a very distinctive punctate distribution (Figure 6B). Treatment with the BrD1-specific inhibitor Olinone did not alter the distribution of eGFP-Brd2wt,

whereas treatment of MS417 induced a punctate distribution of the fusion protein, which resembled that observed in eGFP-Brd2mut-transfected cells (Figure 6B). Taken together, these data suggest that the second BrD of Brd2 is important for its subcellular localization, given that Olinone, which inhibits only the first BrD, did not have any effect on eGFP-Brd2wt, whereas MS417 (inhibiting both the first and second BrDs of Brd2) as well as a mutant Brd2 in both BrDs showed altered nuclear distribution.

The second approach entailed the use of additional chemical probes selective for the inhibition of only the first (MS611) or only of the second (MS765) BrD of BET proteins (Figure S2D; see also the chemical synthesis in the Supplemental Information and Figure S4). Notably, MS765, which is also known as RVX-208, is a compound that was developed by Resverlogix and has been shown to have 15- to 30-fold selectivity for the second BrDs over the first of BET proteins (McLure et al., 2013; Picaud et al., 2013). To investigate whether inhibitors of only the first or second BrD of BET modulated the progression of oligodendrocyte progenitors toward a differentiated phenotype, we characterized the effect of 72 hr treatment with Olinone and MS611 (as inhibitors of the first BrD), MS765/RVX-208 (as an inhibitor of the second BrD), and MS417 (as an inhibitor of both BrDs).

Figure 4. Temporal Control of BrD Inhibition on OPC Differentiation

(A) BrDis do not have broad effects on the expression of oligodendrocytic lineage markers in proliferating conditions. Top: experimental time line. Bottom: qRT-PCR showing the expression levels of differentiation markers after 24 hr of BrDi treatment (Olinone at 1 μ M and MS417 at 0.05 μ M) in the presence of mitogens. Results were normalized to *18S* with relative mRNA levels in DMSO-treated control cells set to 1 ($n = 4$; one-way ANOVA with Dunnett's posttest, *** $p < 0.001$).

(B) Top: different experimental paradigms of BrDi treatment during mOPC differentiation. Bottom: qRT-PCR results showing the transcript levels of late differentiation markers (*Mag*, *Mog*, *Mbp*, and *Plp*) in mOPCs differentiated for 72 hr and treated with BrDi as indicated: (I) during 72 hr or (II) during the first 24 hr of differentiation and then kept in DM with no BrDi. Doses used were 1 μ M Olinone and 0.05 μ M MS417 ($n = 3$; one-way ANOVA with Dunnett's posttest, * $p < 0.05$, ** $p < 0.01$, *** $p < 0.001$).

(C) Top: different experimental paradigms of BrDi treatment. Bottom: qRT-PCR results showing the transcript levels of late differentiation markers (*Mag*, *Mog*, *Mbp*, and *Plp*) in mOPCs differentiated for 72 hr and treated with BrDi as indicated: (I) during 72 hr or (III) during the last 36 hr of differentiation. Doses used were 1 μ M Olinone and 0.05 μ M MS417 ($n = 3$; one-way ANOVA with Dunnett's post test, * $p < 0.05$, ** $p < 0.01$, *** $p < 0.001$). Error bars show \pm SEM.

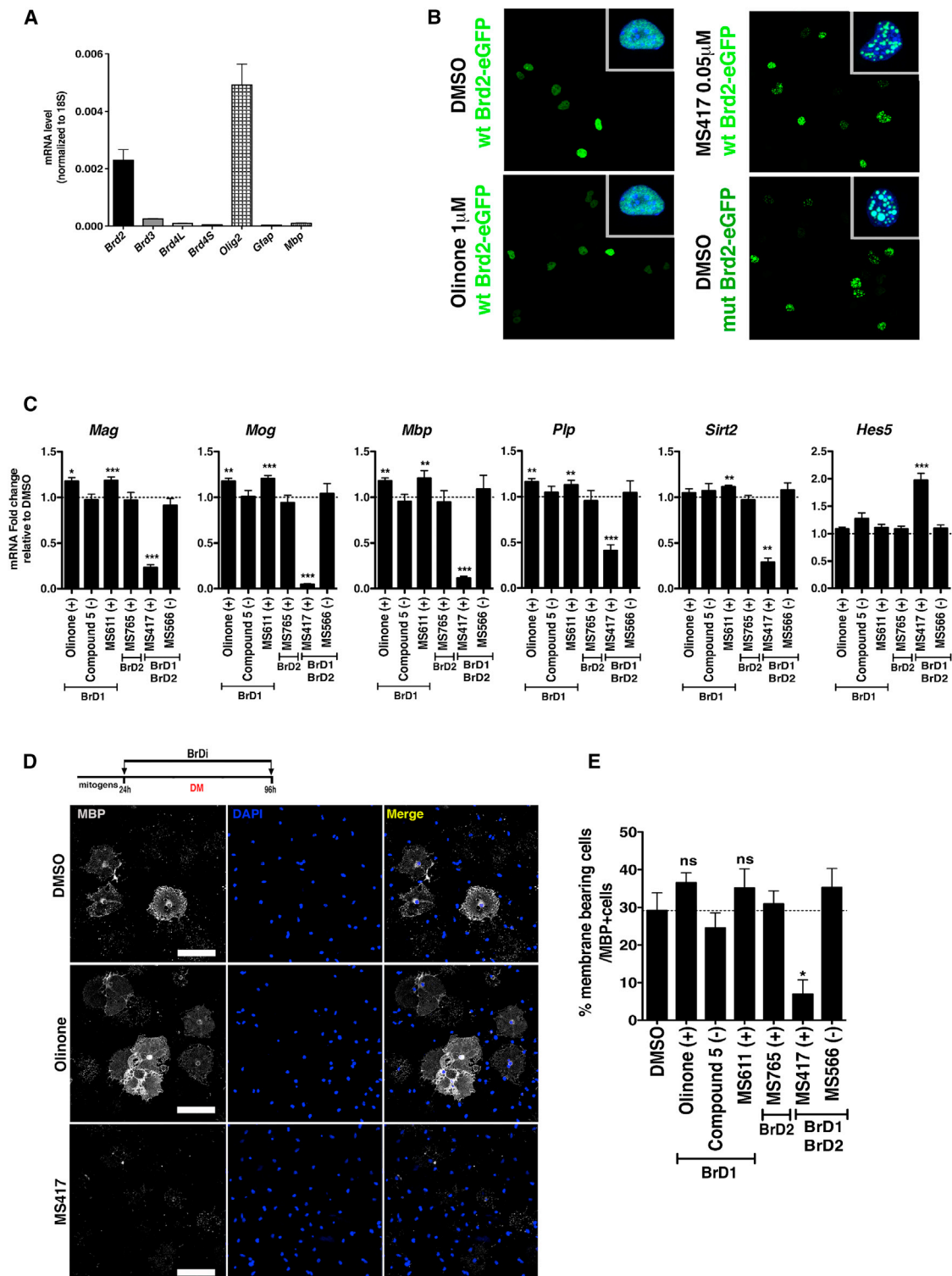


Figure 6. Selective BrDi Inhibition Differentially Affects Brd2 Nuclear Localization and the Progression of Primary OPCs toward a Fully Differentiated Phenotype

(A) qRT-PCR showing the relative expression levels of *Brd2*, *Brd3*, and the long and short isoforms of *Brd4* in primary cultured mOPCs. *Brd2* is the highly expressed isoform in mOPCs. *Olig2* (as a marker of oligodendrocyte lineage), *Mbp* (as a marker of differentiated oligodendrocytes), and *Gfap* (as a marker of astrocytes) levels were also determined as controls. Results were normalized to *18S* ($n = 3$). Error bars show \pm SEM.

(B) Changes in Brd2 nuclear localization after BrDi treatment \pm trichostatin A (TSA). *Olineu* cells were transfected with Brd2-eGFP or mutBrd2-eGFP (with two BrDs mutated) in the presence or absence of BrDi (Olineu 1 μ M, MS417 0.05 μ M); DMSO is used as control. TSA (30 μ M) was added after 24 hr of BrDi treatment

(legend continued on next page)

Differentiation of progenitors into oligodendrocyte was monitored by measuring transcripts for late differentiation genes (*Mag*, *Mog*, *Plp*, and *Mbp*), assessing immunoreactivity for late differentiation markers (MBP⁺/O4⁺) and quantifying the number of membrane-bearing cells. We observed that treatment of Olinone and with the other inhibitor of the first BrD, MS611, increased expression of late differentiation markers (Figure 6C), whereas the inhibitor of the second BrD, MS765/RVX-208, had no effect, and the broad MS417 inhibitor inhibited the expression of these genes (Figure 6C). The number of MBP⁺ membrane-bearing cells (Figure 6D; Figure S5) was similarly increased by Olinone or MS611, unchanged by MS765/RVX-208, and decreased by MS417 treatment (Figure 6E).

Collectively, our results suggest that selective inhibition of the first BrD (such as by Olinone or MS611) facilitates the progression of primary oligodendrocyte progenitors toward a differentiated phenotype, inhibition of the second BrD (such as by MS765/RVX-208) has no effect, and inhibition of both BrDs of BET proteins (such as MS417) negatively affects the differentiation process.

Because of the dynamic nature of lysine acetylation, chemical inhibition of these BrDs may result in lysine deacetylation and subsequent ubiquitination-mediated degradation of the BrD-binding partners. Therefore, chemical inhibition of the two different BrDs is likely to yield distinct functional outcomes. In this study, we compared the effect of a selective inhibitor (Olinone) for the first BrD of BET proteins with that of an inhibitor (MS417) that is equally effective for both BrDs and observed dramatic differences in the biological response of oligodendrocyte progenitors to these treatments. Whereas Olinone promoted differentiation, MS417 inhibited it. This effect was associated with the upregulation of genes such as *E2f1* and *Myc*, which we have shown to be inhibitory for differentiation (Magri et al., 2014a, 2014b) and the downregulation of pro-differentiation genes such as *Cdkn1b* (Zezula et al., 2001). One explanation is that under MS417 treatment, a key transcription factor that is recruited by BET proteins could be degraded in cells, whereas Olinone treatment would leave such a transcription factor intact because of its association with the second BrD of BET proteins. Given the complex nature of gene transcription progression of oligodendrocyte progenitor differentiation, the identification of such a transcription factor(s), and the detailed mechanism of action of chemical inhibition of BET proteins by Olinone and/or MS417 will have to await future investigation. Finally, recent studies show that some kinase inhibitors, such as BI-2536 and TG-101348, developed against PLK1 and JAK2-FLT3 kinases, respectively, have off-target effects

on BrDs in gene activation, including BET BrDs (Ciceri et al., 2014; Ember et al., 2014). Although the reverse may also be possible, this is less likely for Olinone because of its distinct chemical structure from those dual kinase-bromodomain inhibitors. Moreover, similar results obtained with MS611, which shares the same selectivity for the first BrD over the second BrD of BET proteins as that of Olinone, further supports the findings of this study.

SIGNIFICANCE

BET family proteins, through their BrD/acetyl-lysine binding capability, regulate gene transcription in chromatin in multiple steps, including the recruitment of transcription factors to target genes, assembly of the mediator complex at enhancer sites, and activation of paused RNA polymerase II machinery complexes for productive transcriptional elongation (Chiang, 2009). The two BrDs of BET proteins, as shown in BRD3 and BRD4, have context dependent different functions in regulation of ordered gene transcription (Gamsjaeger et al., 2011; Huang et al., 2009; Jang et al., 2005; Lamonica et al., 2011; Schröder et al., 2012; Shi et al., 2014; Yang et al., 2005; Zhang et al., 2012a).

In this study, we highlight the functional importance of chemical modulation of acetylation-mediated protein-protein interactions in transcriptional control of OPC differentiation. We identify Brd2 as the prominent BET expressed in the oligodendrocyte lineage cells. In contrast to what has been reported for other cell types, treatment of oligodendrocyte progenitors with BrDis did not modulate the acetylation of histone H4 and did not affect proliferation. These cells were quite responsive to treatment with selective chemical probes specific for the first, second, or both BrDs of BET proteins. In this functional context, we demonstrate that a small-molecule BrDi, designed to selectively modulate the master chromatin regulators BET proteins, could positively or negatively influence the differentiation of oligodendrocyte progenitors, depending on the targeted BrD. Our data further indicate that a complete chemical inhibition of BET BrD/acetyl-lysine binding activity may possess adverse effects on oligodendrocyte progenitor differentiation, an important step for myelination of axons. Overall, this study opens opportunities for the future development of new therapeutic treatments of demyelinating disorders and also novel chemical agents that could improve the efficiency of the lineage progression of adult stem cells into specialized cell types.

in order to reduce rapid histone acetylation. Cells were fixed at the indicated time points (1 hr of TSA treatment and 6 hr of TSA treatment) (n = 3). The scale bar represents 50 μ m. Error bars show \pm SEM.

(C) Top: experimental timeline. Transcript levels of late differentiation markers (*Mag*, *Mog*, *Mbp*, *Plp*, and *Sirt2*) and the myelin gene transcriptional inhibitor (*Hes5*) in response to 72 hr of BrDi treatment (Olinone at 1 μ M, compound 5 at 1 μ M, MS417 at 0.05 μ M, MS566 at 0.05 μ M, MS611 and MS765/RVX-208 at 0.5 μ M). Results were normalized to *Gapdh* with relative mRNA level in DMSO-treated control cells set to 1 (n = 8; one-way ANOVA with Dunnett's posttest, *p < 0.05, **p < 0.01, ***p < 0.001). Error bars show \pm SEM.

(D) Representative confocal images of mOPCs treated with DMSO, Olinone (1 μ M), and MS417 (0.05 μ M) during 72 hr in DM and stained with MBP antibody (gray) and DAPI (blue). The scale bar represents 100 μ m.

(E) Graph showing the quantification of the percentage of mature MBP⁺ membrane-bearing cells relative to DMSO (n = 3 with 7 or 8 sections per condition; one-way ANOVA with Dunnett's post test, *p < 0.05).

See also Figures S4 and S5.

EXPERIMENTAL PROCEDURES

ITC

Experiments were carried out on a GE MicroCal auto-ITC₂₀₀ instrument at 15°C while stirring at 1,000 rpm in the ITC buffer at pH 7.4, consisting of 50 mM sodium phosphate and 150 mM sodium chloride, as described previously (Zhang et al., 2012a). Compound concentration was determined by NMR and protein concentrations by A₂₈₀ measurements. The protein sample (~75 μM) was placed in the cell, whereas the microsyringe (130 μl) was loaded with a solution of the correspondent compound (0.8 μM) in the ITC buffer. All titrations were conducted using 20 identical injections of 2 μl, with a duration of 4 s per injection and a spacing of 150 s between injections. The heat of dilution was determined by independent titrations (protein into buffer) and was subtracted from the experimental data. The collected data were implemented in the MicroCal Origin software supplied with the instrument to yield enthalpies of binding (ΔH) and binding constants (K_B). Thermodynamic parameters were calculated ($\Delta G = \Delta H - T\Delta S = -RT \ln K_B$, where ΔG , ΔH , and ΔS are the changes in free energy, enthalpy, and entropy of binding, respectively). In all cases, a single binding site model was used.

Protein Crystallization, X-Ray Diffraction Data Collection, and Structure Determination

Purified BRD4-BrD1 protein (14 mg/ml) was mixed with Olinone 4b at a 1:10 molar ratio of protein to ligand. The complex was crystallized using the sitting drop vapor diffusion method at 20°C by mixing 1 μl of protein solution with 1 μl of the reservoir solution, which contains 25% tert-Butanol and 0.1 M Tris-HCl (pH 8.5). Crystals were soaked in the corresponding mother liquor supplemented with 20% ethylene glycerol as a cryoprotectant before freezing in liquid nitrogen. X-ray diffraction data were collected at 100 K at beamline X6A of the National Synchrotron Light Source (NSLS) at Brookhaven National Laboratory. Data were processed using the HKL-2000 suite (Otwinowski and Minor, 1997). The BRD4-BrD1 structure was solved by molecular replacement using the program MOLREP (Vagin and Teplyakov, 1997), and the structure refinement was done using the program Refmac (Murshudov et al., 1997). The graphics program COOT (Emsley and Cowtan, 2004) was used for model building and visualization. Crystal diffraction data and refinement statistics for the structure are displayed in Table S1 (see Supplemental Information).

Primary Oligodendrocytes

OPCs were prepared by sequential immunopanning and kept under undifferentiating conditions, as described previously (Watkins et al., 2008), until the onset of experiments. Briefly, OPCs were isolated from one P6 mouse pup brain using an immunopanning system enabling purity of 95%. The dissected cortex was chopped in papain buffer, incubated for 20 min at 37°C, and titrated in ovomucoid solution (CellSystems). The single-cell solution was centrifuged at 1,000 rpm for 10 min and resuspended in panning buffer and transferred to a bacterial culture plate coated with Anti-BSL1 Griffonia simplicifolia lectin (Vector Labs, L-1100), for negative selection for 15 min, followed by a positive selection step with rat antimouse CD140a (Research Diagnostics, 10R-CD140AMS) as a primary antibody and AffiniPure goat antirat immunoglobulin G (H⁺L) (Dianova, 112-005-003) as a secondary antibody for 45 min. The supernatant was aspirated, and the positive selection plate was washed with Dulbecco's PBS (DPBS). The adherent OPCs were removed using trypsin, centrifuged for 10 min at 1,000 rpm, resuspended in mouse OPC (mOPC) Sato (Watkins et al., 2008), and plated in a T75 culture flask coated with polylysine. The OPCs were cultured in a humidified incubator at 5% CO₂ and 37°C, with media changes every 2 days. OPC were maintained proliferating in the presence of basic fibroblast growth factor (bFGF) (20 ng/ml) and platelet-derived growth factor (PDGF) (10 ng/ml), while oligodendrocyte differentiation was induced by culturing the cells in the absence of mitogens and adding T3 60 nM (Sigma, T5516) to Sato medium.

Olineu Transient Transfection

Olineu cells (15,000 cells/well) were grown on CC2-coated eight-well chambers (Lab-Tek) for all transfection experiments. These cells were transiently transfected using X-tremeGENE 9 DNA transfection reagent (Roche Diagnostics) following the manufacturer's protocol and using equal amounts of the eukaryotic expression vectors pEGFP-C1-Brd2 and pEGFP-C1-Brd2mut

(with both BrDs mutated), previously described by Hnilicová et al. (2013). After 24 hr of transfection, cells were treated for 24 hr with either BrDis (Olinone, MS417) at indicated concentrations or with DMSO as negative control. At this time point, cells were fixed and stained with DAPI (1:10000; Molecular Probes) for immunocytochemistry.

Proliferation Assays

Mouse primarily cultured oligodendrocytes were cultured in CC2-coated eight-well chambers (Lab-Tek) in Sato medium with growth factors (bFGF and PDGF α). Cells were treated with either BrDis at indicated concentrations or DMSO as control for 24 hr. To determine changes in proliferation, cells were fixed and immunolabeled with antibodies against the cell proliferation marker Ki67 (ab14298, 1:1000) for 1 hr at room temperature (RT).

Immunohistochemistry

Immunohistochemistry of cultured cells with O4 antibodies was performed live. Cells were grown on CC2-coated eight-well chambers (Lab-Tek) for all immunocytochemistry. For staining oligodendrocyte lineage markers, cells were rinsed gently with PBS and incubated live with O4 hybridoma supernatant (1:10, gift from Dr. Bansak, University of Connecticut) for 30 min at 37°C. Cells were then fixed with 4% paraformaldehyde (PFA) for 15 min at RT and first incubated with blocking/permeabilization solution (phosphate buffer with gelatin bovine albumin [0.1 M phosphate buffer, 0.1% gelatin, 1% BSA, azide] PGBA plus 10% normal goat serum and 0.5% Triton X-100) for 1 hr at RT. For costaining experiments, cells were incubated with additional primary antibodies against NG2 (Chemicon AB5320, 1:300) and MBP (Covance SMI99, 1:500) overnight at 4°C. A 1 hr incubation with secondary fluorescent antibodies (Alexa Fluor 488 or 546) was performed the following day with counterstaining for DAPI (1:10000; Molecular Probes) to visualize cell nuclei.

Image Acquisition and Quantification

Images were captured at 20 \times and oil immersion 63 \times objective using LSM 710 Metaconfocal laser scanning microscope (Carl Zeiss MicroImaging). For the quantification of the cells at different stages, three fields of each well and four wells of each condition were analyzed, and the immunopositive cells were counted using ImageJ software (NIH). To characterize the 24 hr culture, the proportion of NG2;O4 double positive was calculated by referring to the total number of cells (DAPI+). To characterize the 72 hr culture, the percentage of MBP+ membrane-bearing cells was calculated by dividing the number of each type of cells by the number of total number of cells (DAPI+). OPC proliferation was determined by measuring the mean pixel intensity of DAPI/Ki67+ cells (>99% in each group) relative to DMSO values. One-way ANOVA with Dunnett's multiple-comparison test was performed to assess statistical differences between control and experimental conditions after combing the total number of cells in each group, with a significance threshold of $p < 0.05$.

Acetyl Histone Detection

Olineu cells were plated on 0.1 mg/ml poly-d-lysine (Sigma P7886) coated 96-well plates at a density of 5,000 cells/well. Oligodendrocyte differentiation medium was supplemented with 1% horse serum (Invitrogen 16050). Twenty-four hours after plating, cells were treated with either Olinone at 1 mM or MS417 at 0.05 mM, as well as DMSO as a control for 48 hr. Cells were gently washed with PBS after completion of the treatment and fixed with 4% PFA for 20 min at RT. Cells were then washed and permeabilized with 0.1% triton for 30 min at RT followed by incubation in PGBA plus 10% normal goat serum for 1 hr. Cells were incubated with primary antibodies (H3-Acetyl 1:500 Upstate 06-599; H3AcK14 1:500 Active Motif 39599; H3AcK36 1:1000 Active Motif 39380; H4AcK5 1:2000 Active Motif 39584 and H4AcK12 1:1000 Active Motif 39928) overnight at 4°C. The following day, samples were incubated for 1 hr with secondary fluorescent antibody Alexa Fluor 488 (Invitrogen A11034) and counterstained for DAPI (1:10,000, Molecular Probes). Measurement of the pixel intensity of each primary antibody listed above was accomplished by automated high-throughput screening using plate readers (Perkin Elmer EnVision; TECAN Sapphire and Genios) and high-content microscopes (Molecular Devices ImageXpress Ultra) at the Integrated Screening Core Facility at the Icahn School of Medicine at Mount Sinai. Two-tailed Student's *t* tests were performed to assess statistical differences between the average values in each condition, with a significance threshold of $p < 0.05$.

Cell-Cycle Assay

mOPCs were grown in proliferating conditions until they reached 75% of confluence. At this point, differentiation was induced, and the cells were treated with BrDi as indicated. After 24 to 30 hr of treatment, cells were rinsed twice with DPBS, trypsinized, and pelleted with PBS. One million cells per condition were fixed with cold 70% ethanol overnight. Cell-cycle analysis was performed using the Muse Cell Cycle Analyzer (Millipore, MCH100106) following the manufacturer's protocol.

Statistical Analysis

Unless otherwise stated, all experiments were performed a minimum of three times. The results represent the mean \pm SEM. We compared the data using one-way ANOVA or two-tailed t tests as appropriate and defined statistical significance at $p < 0.05$.

ACCESSION NUMBERS

Structure factors and coordinates for the BRD4 BrD 1 in complex with Olinone are deposited at the Research Collaboratory for Structural Bioinformatics (RCSB) Protein Data Bank under RCSB accession number rcsb085830 and Protein Data Bank (PDB) accession number 4QB3.

SUPPLEMENTAL INFORMATION

Supplemental Information includes Supplemental Experimental Procedures, five figures, and two tables and can be found with this article online at <http://dx.doi.org/10.1016/j.chembiol.2014.05.009>.

AUTHOR CONTRIBUTIONS

G.G.-N., M.G., P.C., and M.-M.Z. conceived and designed the experiments for this study. G.G.-N., G.Z., and Y.R. designed the compounds. G.G.-N. and G.Z. performed the chemical synthesis. A.N.P. and J.J. determine the crystal structure. G.G.-N., L.Z., E.R., and A.V. conducted the biochemical study. M.G. J.K., G.M., and B.M. carried out the molecular and cellular biology experiments. G.G.-N., M.G., P.C., and M.-M.Z. wrote the manuscript.

ACKNOWLEDGMENTS

We acknowledge the use of the NMR facility at the New York Structural Biology Center and the ITC instrument at the High-Throughput Screen Resource Center at Rockefeller University. We also wish to thank the staff at the X6A beamline of the NSLS at Brookhaven National Laboratory for facilitating X-ray data collection. This work was supported in part by the Research Supplements to Promote Diversity in Health-Related Research Program from the National Cancer Institute (G.G.-N.), Clinical and Translational Science Awards grant UL1RR029887 to the Icahn School of Medicine at Mount Sinai, and research grants from the NIH (R03NS072578 to G.G.-N., R37NS42925 and R01NS52738 to P.C., and R01HG004508 and R01CA87658 to M.-M.Z.).

Received: August 29, 2013

Revised: April 28, 2014

Accepted: May 1, 2014

Published: June 19, 2014

REFERENCES

Casaccia-Bonnelil, P., and Liu, A. (2003). Relationship between cell cycle molecules and onset of oligodendrocyte differentiation. *J. Neurosci. Res.* **72**, 1–11.

Chiang, C.M. (2009). Brd4 engagement from chromatin targeting to transcriptional regulation: selective contact with acetylated histone H3 and H4. *F1000 Biol. Rep.* **1**, 98.

Ciceri, P., Müller, S., O'Mahony, A., Fedorov, O., Filippakopoulos, P., Hunt, J.P., Lasater, E.A., Pallares, G., Picaud, S., Wells, C., et al. (2014). Dual kinase-bromodomain inhibitors for rationally designed polypharmacology. *Nat. Chem. Biol.* **10**, 305–312.

Coldham, I., Dobson, B.C., Fletcher, S.R., and Franklin, A.I. (2007). Intramolecular dipolar cycloaddition reactions to give substituted indoles—a formal synthesis of deethylbophyllidine. *Eur. J. Org. Chem.* **16**, 2676–2686.

Dawson, M.A., Prinjha, R.K., Dittmann, A., Giotopoulos, G., Bantscheff, M., Chan, W.I., Robson, S.C., Chung, C.W., Hopf, C., Savitski, M.M., et al. (2011). Inhibition of BET recruitment to chromatin as an effective treatment for MLL-fusion leukaemia. *Nature* **478**, 529–533.

Dhalluin, C., Carlson, J.E., Zeng, L., He, C., Aggarwal, A.K., and Zhou, M.M. (1999). Structure and ligand of a histone acetyltransferase bromodomain. *Nature* **399**, 491–496.

Ember, S.W., Zhu, J.Y., Olesen, S.H., Martin, M.P., Becker, A., Berndt, N., Georg, G.I., and Schonbrunn, E. (2014). Acetyl-lysine binding site of bromodomain-containing protein 4 (BRD4) interacts with diverse kinase inhibitors. *ACS Chem. Biol.* **9**, 1160–1171.

Emsley, P., and Cowtan, K. (2004). Coot: model-building tools for molecular graphics. *Acta Crystallogr. D Biol. Crystallogr.* **60**, 2126–2132.

Filippakopoulos, P., Qi, J., Picaud, S., Shen, Y., Smith, W.B., Fedorov, O., Morse, E.M., Keates, T., Hickman, T.T., Felletar, I., et al. (2010). Selective inhibition of BET bromodomains. *Nature* **468**, 1067–1073.

Filippakopoulos, P., Picaud, S., Mangos, M., Keates, T., Lambert, J.P., Barsyte-Lovejoy, D., Felletar, I., Volkmer, R., Müller, S., Pawson, T., et al. (2012). Histone recognition and large-scale structural analysis of the human bromodomain family. *Cell* **149**, 214–231.

Gamsjaeger, R., Webb, S.R., Lamonica, J.M., Billin, A., Blobel, G.A., and Mackay, J.P. (2011). Structural basis and specificity of acetylated transcription factor GATA1 recognition by BET family bromodomain protein Brd3. *Mol. Cell. Biol.* **31**, 2632–2640.

He, Y., Dupree, J., Wang, J., Sandoval, J., Li, J., Liu, H., Shi, Y., Nave, K.A., and Casaccia-Bonnelil, P. (2007). The transcription factor Yin Yang 1 is essential for oligodendrocyte progenitor differentiation. *Neuron* **55**, 217–230.

Hnilicová, J., Hozefi, S., Stejskalová, E., Dušková, E., Poser, I., Humpolíčková, J., Hof, M., and Staněk, D. (2013). The C-terminal domain of Brd2 is important for chromatin interaction and regulation of transcription and alternative splicing. *Mol. Biol. Cell* **24**, 3557–3568.

Huang, B., Yang, X.D., Zhou, M.M., Ozato, K., and Chen, L.F. (2009). Brd4 coactivates transcriptional activation of NF- κ B via specific binding to acetylated RelA. *Mol. Cell. Biol.* **29**, 1375–1387.

Jang, M.K., Mochizuki, K., Zhou, M., Jeong, H.S., Brady, J.N., and Ozato, K. (2005). The bromodomain protein Brd4 is a positive regulatory component of P-TEFb and stimulates RNA polymerase II-dependent transcription. *Mol. Cell* **19**, 523–534.

Lamonica, J.M., Deng, W., Kadauke, S., Campbell, A.E., Gamsjaeger, R., Wang, H., Cheng, Y., Billin, A.N., Hardison, R.C., Mackay, J.P., and Blobel, G.A. (2011). Bromodomain protein Brd3 associates with acetylated GATA1 to promote its chromatin occupancy at erythroid target genes. *Proc. Natl. Acad. Sci. USA* **108**, E159–E168.

Magri, L., Gacias, M., Wu, M., Swiss, V.A., Janssen, W.G., and Casaccia, P. (2014a). c-Myc-dependent transcriptional regulation of cell cycle and nucleosomal histones during oligodendrocyte differentiation. *Neuroscience*. Published online February 4, 2014. <http://dx.doi.org/10.1016/j.neuroscience.2014.01.051>.

Magri, L., Swiss, V.A., Jablonska, B., Lei, L., Pedre, X., Walsh, M., Zhang, W., Gallo, V., Canoll, P., and Casaccia, P. (2014b). E2F1 coregulates cell cycle genes and chromatin components during the transition of oligodendrocyte progenitors from proliferation to differentiation. *J. Neurosci.* **34**, 1481–1493.

Marin-Husstege, M., Muggironi, M., Liu, A., and Casaccia-Bonnelil, P. (2002). Histone deacetylase activity is necessary for oligodendrocyte lineage progression. *J. Neurosci.* **22**, 10333–10345.

McLure, K.G., Gesner, E.M., Tsujikawa, L., Kharenko, O.A., Atwell, S., Campeau, E., Wasiak, S., Stein, A., White, A., Fontano, E., et al. (2013). RVX-208, an inducer of ApoA-I in humans, is a BET bromodomain antagonist. *PLoS ONE* **8**, e83190.

- Murshudov, G.N., Vagin, A.A., and Dodson, E.J. (1997). Refinement of macromolecular structures by the maximum-likelihood method. *Acta Crystallogr. D Biol. Crystallogr.* *53*, 240–255.
- Nicodeme, E., Jeffrey, K.L., Schaefer, U., Beinke, S., Dewell, S., Chung, C.W., Chandwani, R., Marazzi, I., Wilson, P., Coste, H., et al. (2010). Suppression of inflammation by a synthetic histone mimic. *Nature* *468*, 1119–1123.
- Otwinowski, Z., and Minor, W. (1997). Processing of X-ray diffraction data collected in oscillation mode. In *Methods in Enzymology*, C.W. Carter, Jr., ed. (San Diego, CA: Academic Press), pp. 307–326.
- Picaud, S., Wells, C., Felletar, I., Brotherton, D., Martin, S., Savitsky, P., Diez-Dacal, B., Philpott, M., Bountra, C., Lingard, H., et al. (2013). RVX-208, an inhibitor of BET transcriptional regulators with selectivity for the second bromodomain. *Proc. Natl. Acad. Sci. USA* *110*, 19754–19759.
- Puissant, A., Frumm, S.M., Alexe, G., Bassil, C.F., Qi, J., Chanthery, Y.H., Nekritz, E.A., Zeid, R., Gustafson, W.C., Greninger, P., et al. (2013). Targeting MYCN in neuroblastoma by BET bromodomain inhibition. *Cancer Disc.* *3*, 308–323.
- Rodriguez, J.-G., and Temprano, F.J. (1989). Synthesis of 4-(N,N-dimethylaminoethyl)-1,2,3,4-tetrahydrocarbazole: molecular structure and reactivity of the 1,2-dihydrocarbazol-4(3H)-one and derivatives. *J. Chem. Soc. Perkin Trans. I*, 2117–2122.
- Sachchidanand, Resnick-Silverman, L., Yan, S., Mutjaba, S., Liu, W.J., Zeng, L., Manfredi, J.J., and Zhou, M.M. (2006). Target structure-based discovery of small molecules that block human p53 and CREB binding protein association. *Chem. Biol.* *13*, 81–90.
- Sanchez, R., and Zhou, M.M. (2009). The role of human bromodomains in chromatin biology and gene transcription. *Curr. Opin. Drug Discov. Devel.* *12*, 659–665.
- Schröder, S., Cho, S., Zeng, L., Zhang, Q., Kaehlcke, K., Mak, L., Lau, J., Bisgrove, D., Schnölzer, M., Verdin, E., et al. (2012). Two-pronged binding with bromodomain-containing protein 4 liberates positive transcription elongation factor b from inactive ribonucleoprotein complexes. *J. Biol. Chem.* *287*, 1090–1099.
- Shen, S., Li, J., and Casaccia-Bonnel, P. (2005). Histone modifications affect timing of oligodendrocyte progenitor differentiation in the developing rat brain. *J. Cell Biol.* *169*, 577–589.
- Shen, S., Sandoval, J., Swiss, V.A., Li, J., Dupree, J., Franklin, R.J., and Casaccia-Bonnel, P. (2008). Age-dependent epigenetic control of differentiation inhibitors is critical for remyelination efficiency. *Nat. Neurosci.* *11*, 1024–1034.
- Shi, J., Wang, Y., Zeng, L., Wu, Y., Deng, J., Zhang, Q., Lin, Y., Li, J., Kang, T., Tao, M., et al. (2014). Disrupting the interaction of BRD4 with diacetylated Twist suppresses tumorigenesis in basal-like breast cancer. *Cancer Cell* *25*, 210–225.
- Swiss, V.A., and Casaccia, P. (2010). Cell-context specific role of the E2F/Rb pathway in development and disease. *Glia* *58*, 377–390.
- Vagin, A., and Teplyakov, A. (1997). MOLREP: an automated program for molecular replacement. *J. Appl. Crystallogr.* *30*, 1022–1025.
- Watkins, J., Basu, S., and Bogenhagen, D.F. (2008). A quantitative proteomic analysis of mitochondrial participation in p19 cell neuronal differentiation. *J. Proteome Res.* *7*, 328–338.
- Wu, M., Hernandez, M., Shen, S., Sabo, J.K., Kelkar, D., Wang, J., O’Leary, R., Phillips, G.R., Cate, H.S., and Casaccia, P. (2012). Differential modulation of the oligodendrocyte transcriptome by sonic hedgehog and bone morphogenetic protein 4 via opposing effects on histone acetylation. *J. Neurosci.* *32*, 6651–6664.
- Yang, Z., Yik, J.H., Chen, R., He, N., Jang, M.K., Ozato, K., and Zhou, Q. (2005). Recruitment of P-TEFb for stimulation of transcriptional elongation by the bromodomain protein Brd4. *Mol. Cell* *19*, 535–545.
- Ye, F., Chen, Y., Hoang, T., Montgomery, R.L., Zhao, X.H., Bu, H., Hu, T., Taketo, M.M., van Es, J.H., Clevers, H., et al. (2009). HDAC1 and HDAC2 regulate oligodendrocyte differentiation by disrupting the beta-catenin-TCF interaction. *Nat. Neurosci.* *12*, 829–838.
- Zezula, J., Casaccia-Bonnel, P., Ezhevsky, S.A., Osterhout, D.J., Levine, J.M., Dowdy, S.F., Chao, M.V., and Koff, A. (2001). p21cip1 is required for the differentiation of oligodendrocytes independently of cell cycle withdrawal. *EMBO Rep.* *2*, 27–34.
- Zhang, G., Liu, R., Zhong, Y., Plotnikov, A.N., Zhang, W., Zeng, L., Rusinova, E., Gerona-Nevarro, G., Moshkina, N., Joshua, J., et al. (2012a). Down-regulation of NF- κ B transcriptional activity in HIV-associated kidney disease by BRD4 inhibition. *J. Biol. Chem.* *287*, 28840–28851.
- Zhang, W., Prakash, C., Sum, C., Gong, Y., Li, Y., Kwok, J.J., Thiessen, N., Pettersson, S., Jones, S.J., Knapp, S., et al. (2012b). Bromodomain-containing protein 4 (BRD4) regulates RNA polymerase II serine 2 phosphorylation in human CD4+ T cells. *J. Biol. Chem.* *287*, 43137–43155.
- Zhang, G., Plotnikov, A.N., Rusinova, E., Shen, T., Morohashi, K., Joshua, J., Zeng, L., Mujtaba, S., Ohlmeyer, M., and Zhou, M.M. (2013). Structure-guided design of potent diazobenzene inhibitors for the BET bromodomains. *J. Med. Chem.* *56*, 9251–9264.
- Zuber, J., Shi, J., Wang, E., Rappaport, A.R., Herrmann, H., Sison, E.A., Magoon, D., Qi, J., Blatt, K., Wunderlich, M., et al. (2011). RNAi screen identifies Brd4 as a therapeutic target in acute myeloid leukaemia. *Nature* *478*, 524–528.